Composites: Part A

Effects of exposure time and intensity on the shot peen forming characteristics of Ti/CFRP laminates

Yubing Hu [a,d], Wei Zhang [b], Wei Jiang [b], Liang Cao [b], Yizhou Shen [a], Huaguan Li [a], Zhongwei Guan [d], Jie Tao [a,c,*], Jiang Xu [a]

[a] College of Material Science and Technology, Nanjing University of Aeronautics and Astronautics, 210016 Nanjing, China
[b] Main Plant of Machining, Xi'an Aircraft Industry Company LTD., 710089 Xi'an, China
[c] Jiangsu Collaborative Innovation Center for Advanced Inorganic Function Composites, China
[d] School of Engineering, University of Liverpool, L69 3GH Liverpool, UK

ARTICLE INFO

Article history:
Received 15 June 2016
Received in revised form 11 September 2016
Accepted 29 September 2016
Available online 30 September 2016

Keywords:
Hybrid
Laminate
Peen forming
Fibre metal laminates

ABSTRACT

Fibre metal laminates (FMLs) have been developed as promising materials in the manufacture of aircrafts. In order to reduce costs during the manufacture process, relatively new forming techniques are required. In this work, shot peen forming process was performed on Ti/CFRP laminates. Additionally, effects of shot peening parameters on the forming characteristic of Ti/CFRP laminates were investigated. The results showed that the peening coverage and the final arc height of the FML strip were increased with the extension of the exposure time. Similarly, the final arc height of the FML strip increased linearly with the augment of the applied Almen intensity. Moreover, FML with different lay-ups showed diverse forming characteristics. It was more difficult to generate the bending deformation in the FML made with unidirectional lay-up prepreg. Finally, an improvement in tensile properties of the FMLs was confirmed after the shot peening treatment.

1. Introduction

Fibre metal laminates (FMLs) are super hybrid materials composed by thin metal layers and fibre reinforced polymer layers. As a family of super hybrid composites, FMLs possess the features that both metal and fibre reinforced composite have, such as high specific strength and stiffness, lightweight, excellent impact resistance and superb fatigue properties [1–5]. With these outstanding characteristics, FMLs have been developed rapidly since they were first introduced by Delft University later in 1970s.

There are several groups of FMLs which are known as Arall (Aramid fibre/Aluminum), Glare (Glass fibre/Aluminum), Carall (Carbon fibre/Aluminum) and TiGr (Graphite fibre/Titanium). At present, Arall has been used as the cargo door of the C-17 and Glare has been successfully utilized in manufacturing the upper fuselage of the Airbus 380 aircraft [6–11]. With the development of the aerospace industry, the aircrafts are being designed to fly faster and to last longer than ever before [12]. Obviously, the skin of the aircrafts will experience a high temperature profile during their service process. Hence, TiGr laminates can be candidate materials for next generation aircrafts owning to their excellent high temperature performance.

During the manufacturing process of the aircraft, there are roughly two steps: the creation of the parts and assembly of the parts into the structure. It is necessary to find effective methods to form the FMLs before assembling. However, compared with sheet metal forming, composite forming is a relatively new area for researchers. Normally, there are two different approaches to obtain a complicated shape of FML parts, as shown in Fig. 1. It can be achieved by deforming the metal layers and thereafter make laminates from the individual plies. However, pre-forming of the thin metal sheets before laminating is not merely difficult but expensive. Hence, it is attractive to reduce the process cycle and labor cost by a forming curved shape of FML plates.

Kalyanasundaram et al. [13] investigated the stamp forming behavior of self reinforced-PP based fibre metal laminates. They studied the effects of temperature, binder force, feed rate and interaction effects on major strain and strain ratios (minor strain/-major strain). However, it was concluded that only the factors such as temperature and binder force affect the major strain and strain ratios significantly. Dou et al. [14,15] simulated the stamping process of fibre metal laminates by using finite element modeling. Two FMLs made with different prepreg types were investigated in their work. It was confirmed that properties of core composite

* Corresponding author at: College of Material Science and Technology, Nanjing University of Aeronautics and Astronautics, 210016 Nanjing, China.
E-mail addresses: huyubing@nuaa.edu.cn (Y. Hu), taojie@nuaa.edu.cn (J. Tao).

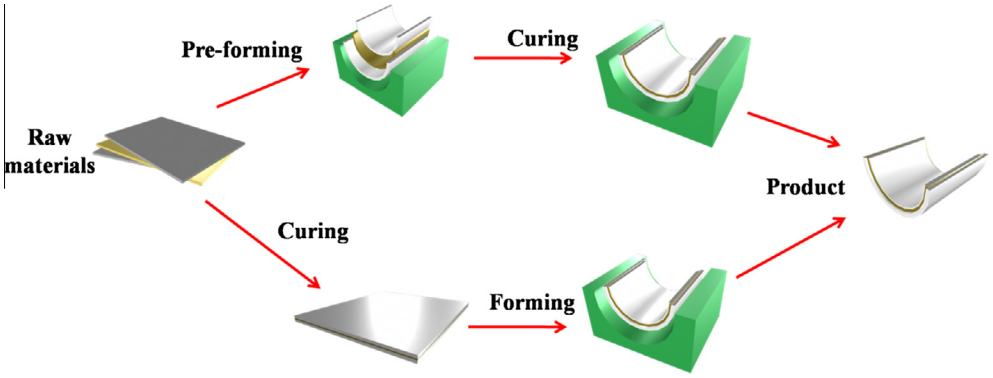

Fig. 1. Two technical routes to create a FMLs product. (For interpretation of the references to colour in this figure legend, the reader is referred to the web version of this article.)

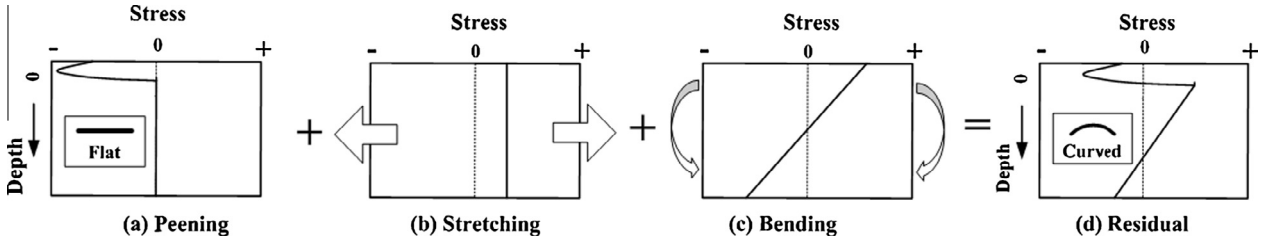

Fig. 2. Balancing of (a) induced stresses through, (b) elongation and (c) bending of the part to reach an equilibrated, (d) residual stress profile.

layers projected strong influences on the forming behavior of the FMLs. Moreover, several manufacture processes and forming methods were reviewed by Sinke [16]. He introduced the roll bending forming process and stretch forming process in the paper. Also, failure modes and forming limit of FMLs were presented. Although traditional methods have been successfully utilized to manufacture FML products, novel forming approaches with advantages of high productivity, low labor cost and dimension stability are still yet to be developed.

Shot peen forming is a manufacturing method which is commonly used in aerospace industry, especially used for forming the contoured integral aircraft skin panels. During the shot peening process, the surface of the metal sheet is mechanically treated by the stream of small hard shot with sufficient kinetic energy. Therefore, the outer layer of the metal sheet surface is plastically deformed, introducing the compressive stresses in the surface through the thickness direction. In order to balance the compressive stresses, the thin outer layer has to be stretched along the surface which produces significant bending, as schematically shown in Fig. 2 [17]. As a promising forming method, shot peen forming has been investigated by numerous researchers. Hong et al. [18] applied a numerical simulation of the shot peening process and successfully obtained the relationships between peening process parameters and peening quality. Quantitative relationships between the saturation, surface coverage and roughness with respect to peening time were established by Miao et al. [19]. Moreover, Russig et al. [20] undertook some pre-study on shot peening forming on FMLs. They investigated the possibilities to form Glare by using shot peen forming. It was proved that Glare possessed a similar deformation behavior with monolithic sheets under quasi-static indentation with single steel balls. Additionally, Glare parts with curvature radius less than 2500 mm could be obtained without damage.

The aim of this work is to experimentally investigate the effects of two important shot peening parameters (exposure time and Almen intensity) on the forming characteristics of Ti/CFRP laminates. Ti/CF/Polyimide FMLs and Ti/CF/PEEK FMLs were prepared and selected as the research objects. Shot peening experiments were carried out on the FML strips under different exposure time durations (0.76, 1, 3, 5 and 7 s) and different Almen intensities (0.097, 0.133, 0.156 and 0.193 mmA). The relationship between the curvature radius and the peening parameters was obtained after experimental and theoretical investigation.

2. Experimental procedure

2.1. Materials

Titanium plates with a thickness of 0.3 mm (BAOJI Titanium Industry Co., Ltd. China), carbon fibre (TR50S 6K, Mitsubishi Rayon Co., Ltd., Japan), PMR polyimide resin (KH-308, Institute of Chemistry, Chinese Academy of Science) and carbon fibre reinforced PEEK prepreg (APC-2, Ten Cate nv.) was used as constituent materials. The PMR polyimide contains 50 wt.% of polymerized reaction mixtures. Carbon fibre reinforced polyimide prepreg was self-prepared by numerically controlled automatic placement machine in a laboratory in Nanjing University of Aeronautics and Astronautics. Two series of FMLs, Ti/CF/Polyimide FMLs and Ti/CF/PEEK FMLs, were prepared according to the consolidating processes reported in [4,21]. The detailed information of the FMLs used in this work is listed in Table 1.

Table 1
Detail information of the FMLs specimens.

Code	Configuration	Thickness (mm)	Tensile strength (MPa)	Modulus (GPa)
PI-U	[Ti/0/0/Ti/0/0/Ti]	1.45 ± 0.12	938 ± 11	105 ± 8
PI-C	[Ti/0/90/Ti/90/0/Ti]	1.46 ± 0.11	633 ± 14	83 ± 7
PEEK-U	[Ti/0/0/Ti/0/0/Ti]	1.49 ± 0.09	935 ± 12	101 ± 10
PEEK-C	[Ti/0/90/Ti/90/0/Ti]	1.48 ± 0.07	621 ± 27	83 ± 6

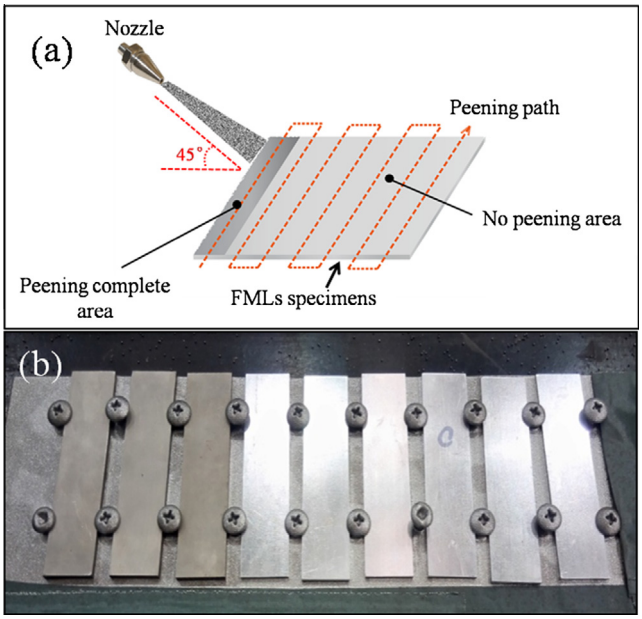

Fig. 3. (a) Schematic diagram of the peening process, (b) specimens support scheme. (For interpretation of the references to colour in this figure legend, the reader is referred to the web version of this article.)

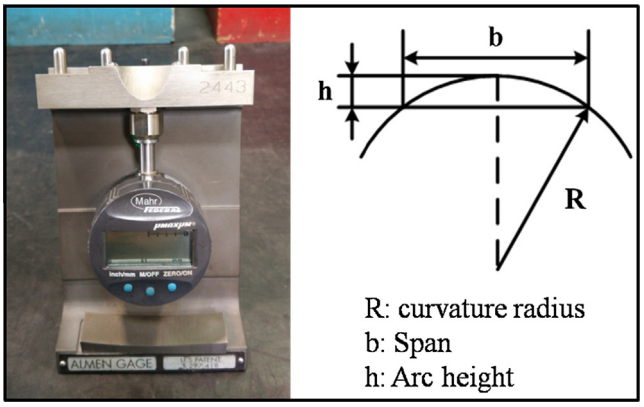

Fig. 4. Almen gauge and schematic of the curvature radius. (For interpretation of the references to colour in this figure legend, the reader is referred to the web version of this article.)

2.2. Shot peening experiments

Shot peening experiments were performed on the Sisson Lehmann MP4000 setup and utilized the AZB425 ceramic shots (diameters ranging from 425 to 600 μm [22]) as the peening medium. The nozzle with a diameter of 10 mm was mounted on an industrial robot. During the shot peening process, test specimens were placed 500 mm away from the peening nozzle and oriented 45° to the shot stream. Peening process was carried out in a single pass following a zig-zag path of parallel lines with a step-over distance of 10 mm, as illustrated in Fig. 3. Strips with dimensions of 76 mm × 19 mm were cut from the FMLs by using wire electrical discharge machining (WEDM) technique. Tensile specimens with dimensions of 200 mm × 12.5 mm were also obtained.

Shot peening experiments were performed under different conditions to understand the relationship between the peening parameters and the forming results. Two control factors, i.e. exposure time and Almen intensity, were considered. Shot peening experiments were performed under different exposure time durations (0.76, 1, 3, 5 and 7 s) and different Almen intensities (0.097, 0.133, 0.156 and 0.193 mmA). Moreover, the effects of shot peening on the tensile properties of the specimens were assessed. Tensile specimens were shot peened in both sides under certain Almen intensity (0.097 and 0.156 mmA) to avoid bending deformation.

2.3. Characterizations of deformation, surface morphologies and mechanical property

The deformation of the specimen induced by shot peening was evaluated with arc height measured by using an Almen gauge. Two specimens were tested for each case and the average values were obtained. Considering the spring-back problem which can be generated during the forming process, arc heights of the specimens were measured after shot peening and one month later respectively. However, these two values show no discernible difference, indicating the stability of the specimens after shot peening. Hence, the results discussed in Section 3 were obtained from specimens after one month long seasoning.

The relationship between the curvature radius R and the arc height h can be obtained by a geometrical analysis, as schematically displayed in Fig. 4, which is expressed by Eq. (1) below

$$R^2 = \left(\frac{b}{2}\right)^2 + (R-h)^2 \tag{1}$$

Table 2
Peening parameters and results (different exposure time).

Category	FMLs type	Exposure time (s)	Arc height (mm)	Curvature radius (mm)
PI-U	[Ti/0/0/Ti/0/0/Ti]	0.76	0.131 ± 0.002	962 ± 14
		1	0.135 ± 0.001	933 ± 17
		3	0.219 ± 0.012	577 ± 21
		5	0.249 ± 0.015	517 ± 21
		7	0.266 ± 0.022	476 ± 40
PI-C	[Ti/0/90/Ti/90/0/Ti]	0.76	0.110 ± 0.003	1146 ± 31
		1	0.125 ± 0.005	1009 ± 40
		3	0.241 ± 0.008	523 ± 17
		5	0.313 ± 0.020	404 ± 26
		7	0.345 ± 0.012	366 ± 13
PEEK-U	[Ti/0/0/Ti/0/0/Ti]	0.76	0.119 ± 0.002	1059 ± 16
		1	0.131 ± 0.006	963 ± 35
		3	0.244 ± 0.011	517 ± 23
		5	0.281 ± 0.010	448 ± 15
		7	0.292 ± 0.016	432 ± 21
PEEK-C	[Ti/0/90/Ti/90/0/Ti]	0.76	0.157 ± 0.001	802 ± 5
		1	0.179 ± 0.007	705 ± 27
		3	0.268 ± 0.013	471 ± 23
		5	0.345 ± 0.014	365 ± 15
		7	0.387 ± 0.022	327 ± 18

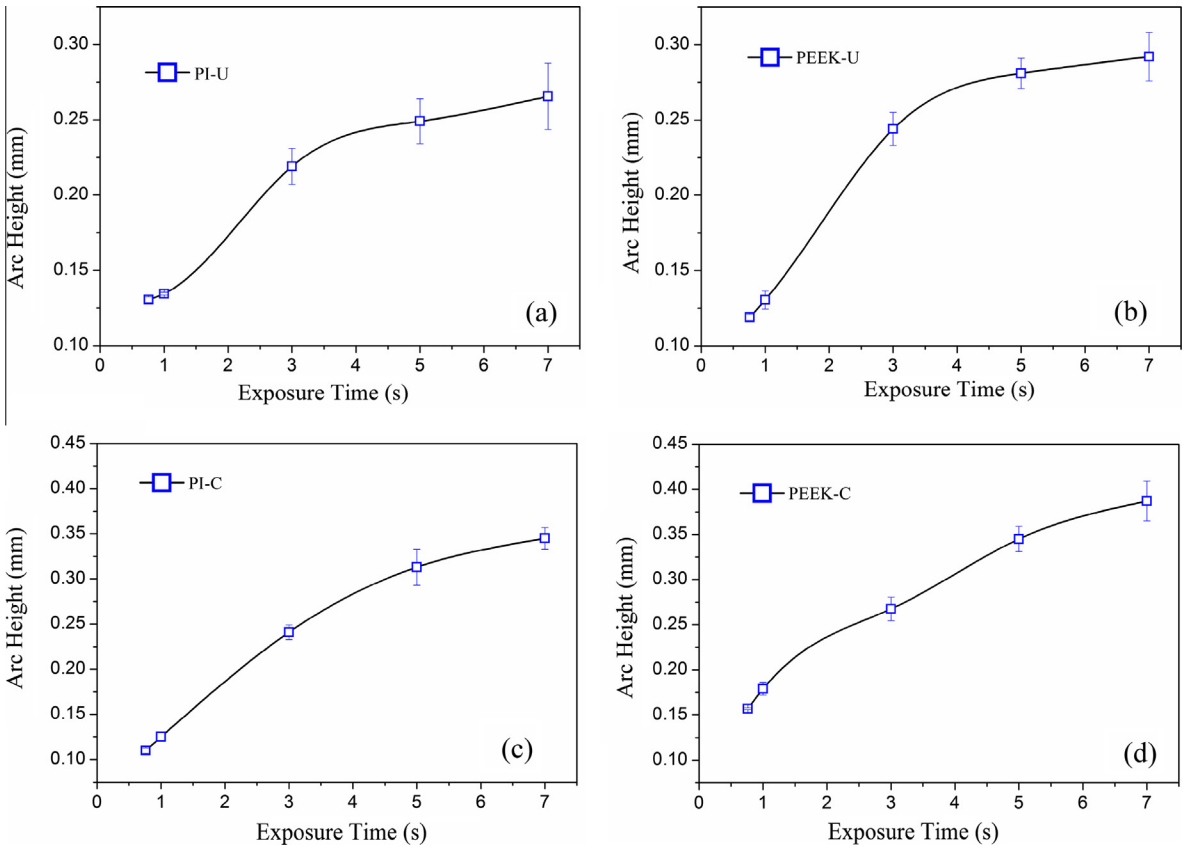

Fig. 5. Experimental relationship between the arc height and the exposure time: (a) PI-U, (b) PEEK-U, (c) PI-C, (d) PEEK-C. (For interpretation of the references to colour in this figure legend, the reader is referred to the web version of this article.)

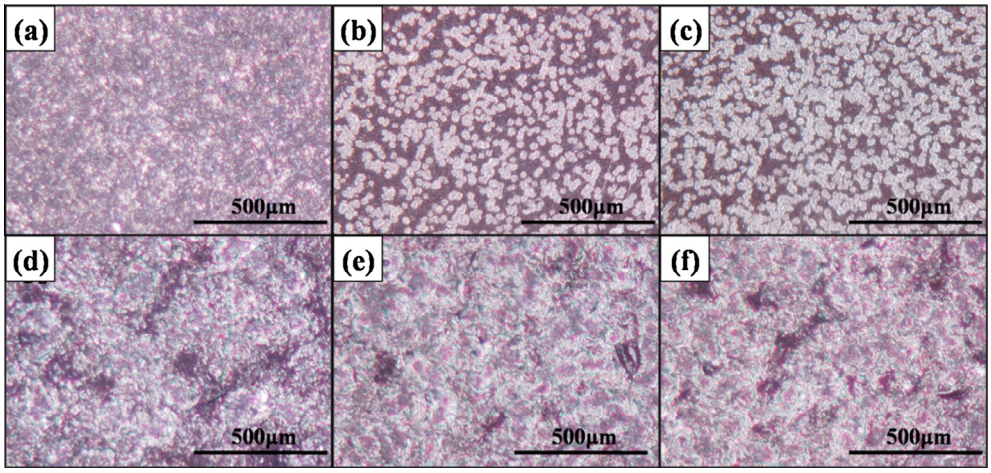

Fig. 6. 2D topographies of the surfaces after peening for different time: (a) origin sample, (b) 0.76 s, (c) 1 s, (d) 3 s, (e) 5 s, (f) 7 s. (For interpretation of the references to colour in this figure legend, the reader is referred to the web version of this article.)

where b refers to the length of the span, which is equal to 31.75 mm in this study. Since $h \ll R$, Eq. (1) can be rewritten as

$$R = \frac{b^2}{8h} \tag{2}$$

Therefore, the curvature radius of the specimen can be obtained according to Eq. (2).

3D microscope (Leica DVM 5000) was employed to observe the morphologies of the specimens. Tensile properties of the specimens after peening were assessed on a SANS CMT 5105 microcomputer-controlled electronic universal testing machine according to the ASTM D3039M.

3. Results and discussion

3.1. Different exposure time

The relationships between the resulted arc heights and the exposure time are present in Table 2 and Fig. 5. It is clear that different types of strips exhibit the similar variation tendency of

the arc height from Fig. 5(a)–(d). Arc height produced by the residual stresses increases almost linearly with the exposure time initially. Then, the slopes of the curves decrease, indicating the saturation of the peening. Smaller curvature radius strips are obtained after shot peened for a longer time, as expected. Meanwhile, the curvature radii of the strips are found less than 1200 mm, which are sufficient to form fuselage components for the A380 airplane [20].

During the peening process, exposure time is considered as an extremely important parameter for the forming results and surface quality with the different peening coverage. It is observed that more random indentations are produced with the extension of exposure time, which causes the increase of the peening coverage, as shown in Fig. 6. The peening coverages of the specimens with different exposure time (0.76, 1, 3, 5 and 7 s) evaluated by the ImageJava software are 47.4, 52.1, 79.7, 96.3 and 99.7%, respectively. Moreover, surface roughness is a crucial property of metallic materials after shot peening treatment according to its effects on fatigue strength and corrosion resistance [23]. Fig. 7 presents the relationship between surface roughness (Ra) and coverage with different peening conditions. It is noted that the increased percentage of the coverage causes an augment in the surface roughness degree initially according to the more shot impact on the surface. The surface topographies of the specimens are displayed in Fig. 8, indicating the complex surface structures after shot peening. However, the degree of the surface roughness reaches a platform with the increase of percentage of the coverage. Finally, the surface roughness value decreases slightly. It can be deduced that with increasing the percentage of coverage, the surface is much more homogeneous after shot impact under certain Almen intensity. In other words, increasing coverage is an effective approach to reduce the surface roughness to some extent.

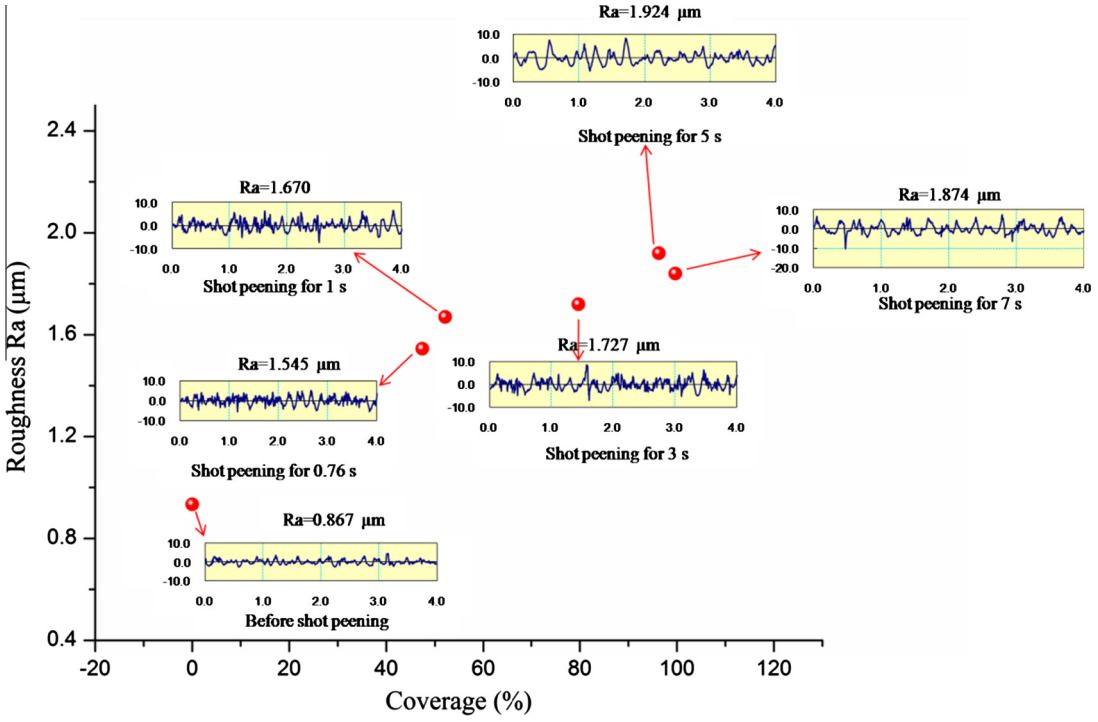

Fig. 7. Surface roughness (Ra) vs. coverage. (For interpretation of the references to colour in this figure legend, the reader is referred to the web version of this article.)

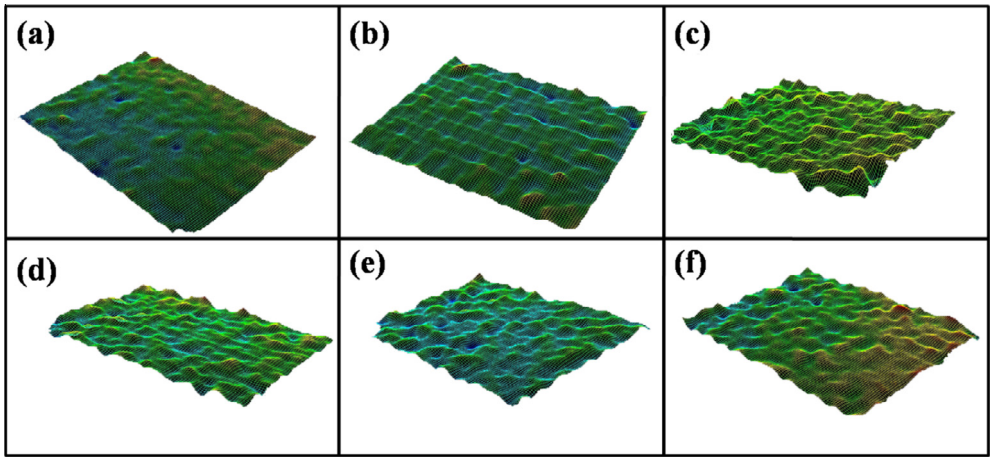

Fig. 8. Surface topography obtained by 3D microscope: (a) origin sample, (b) 0.76 s (c) 1 s, (d) 3 s, (e) 5 s, (f) 7 s. (For interpretation of the references to colour in this figure legend, the reader is referred to the web version of this article.)

Table 3
Peening parameters and results (different Almen intensity).

Category	FMLs type	Almen intensity (mmA)	Arc height (mm)	Curvature radius (mm)
PI-U	[Ti/0/0/Ti/0/0/Ti]	0.097	0.139 ± 0.001	906 ± 6
		0.133	0.190 ± 0.009	664 ± 33
		0.156	0.249 ± 0.011	507 ± 22
		0.193	0.342 ± 0.013	368 ± 14
PI-C	[Ti/0/90/Ti/90/0/Ti]	0.097	0.169 ± 0.007	746 ± 29
		0.133	0.258 ± 0.013	489 ± 25
		0.156	0.291 ± 0.019	434 ± 28
		0.193	0.422 ± 0.012	290 ± 8
PEEK-U	[Ti/0/0/Ti/0/0/Ti]	0.097	0.143 ± 0.015	855 ± 45
		0.133	0.184 ± 0.009	686 ± 34
		0.156	0.281 ± 0.019	450 ± 30
		0.193	0.347 ± 0.013	363 ± 13
PEEK-C	[Ti/0/90/Ti/90/0/Ti]	0.097	0.200 ± 0.011	631 ± 30
		0.133	0.267 ± 0.012	472 ± 20
		0.156	0.321 ± 0.015	393 ± 22
		0.193	0.492 ± 0.021	256 ± 11

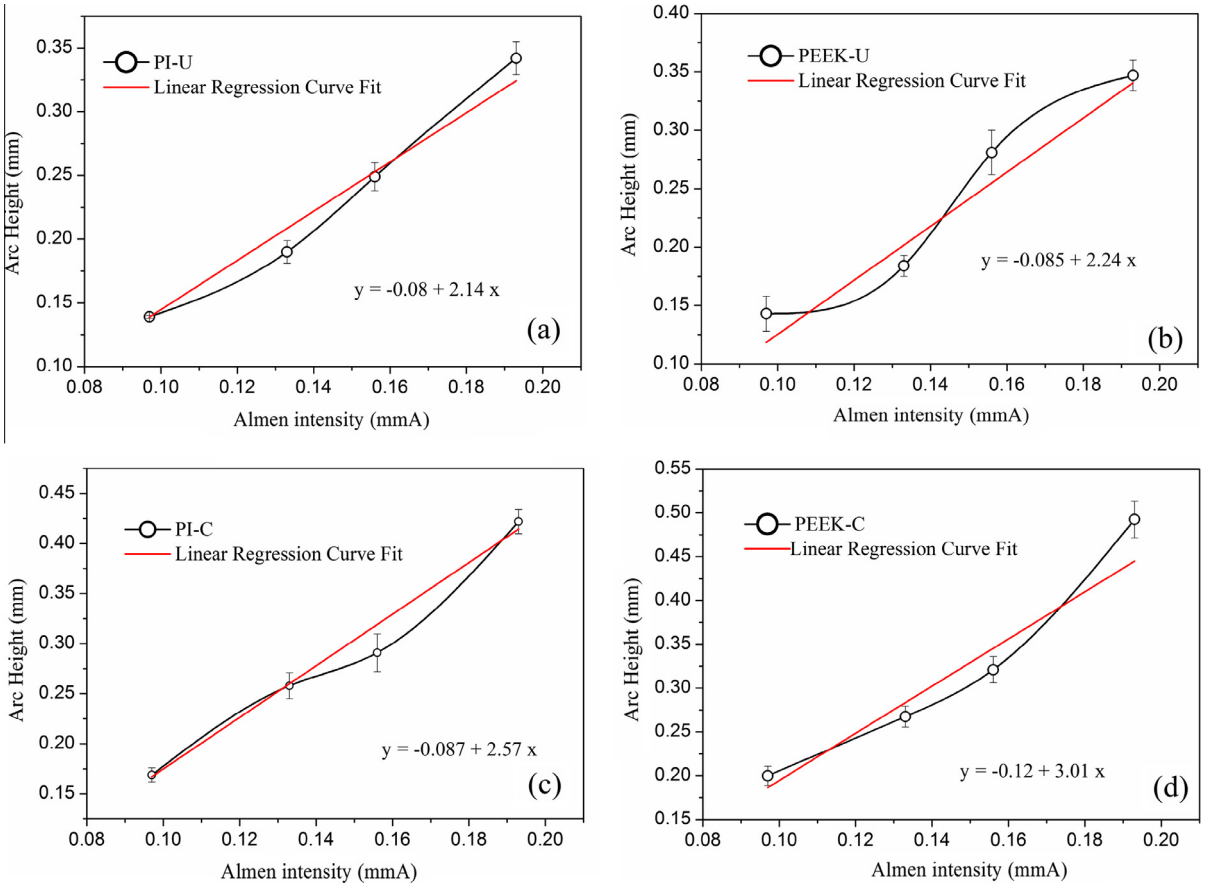

Fig. 9. Experimental relationship between arc height and Almen intensity: (a) PI-U, (b) PEEK-U, (c) PI-C, (d) PEEK-C. (For interpretation of the references to colour in this figure legend, the reader is referred to the web version of this article.)

3.2. Different Almen intensity

In order to recognize the effects of Almen intensity on the peening results, relevant experiments were carried out by using the parameters presented in Table 3. All strips were visually examined after peening to assure that 100% coverage was achieved. It is observed in Table 3 that the arc height of the sample is increased when a higher Almen intensity is employed during the shot peening process. Also, FMLs with different lay-ups present various responses to the shot peening process, no matter Ti/CF/Polyimide FMLs or Ti/CF/PEEK FMLs. In order to show the tendency more evidently, the results are collected in Fig. 9.

Fig. 9 illustrates the relationship between the Almen intensity and the resulted arc height. Similar tendency is found in different specimens in which arc heights of the strips are increased linearly with the increase of Almen intensity. The correlation between the Almen intensity and the arc height of different strips after shot peening is described in Eqs. (3)–(6) respectively, as determined from fitted linear regression curves.

$$Arc\ height\ (h_{PI-U}) = 2.14\ intensity - 0.08 \quad (3)$$

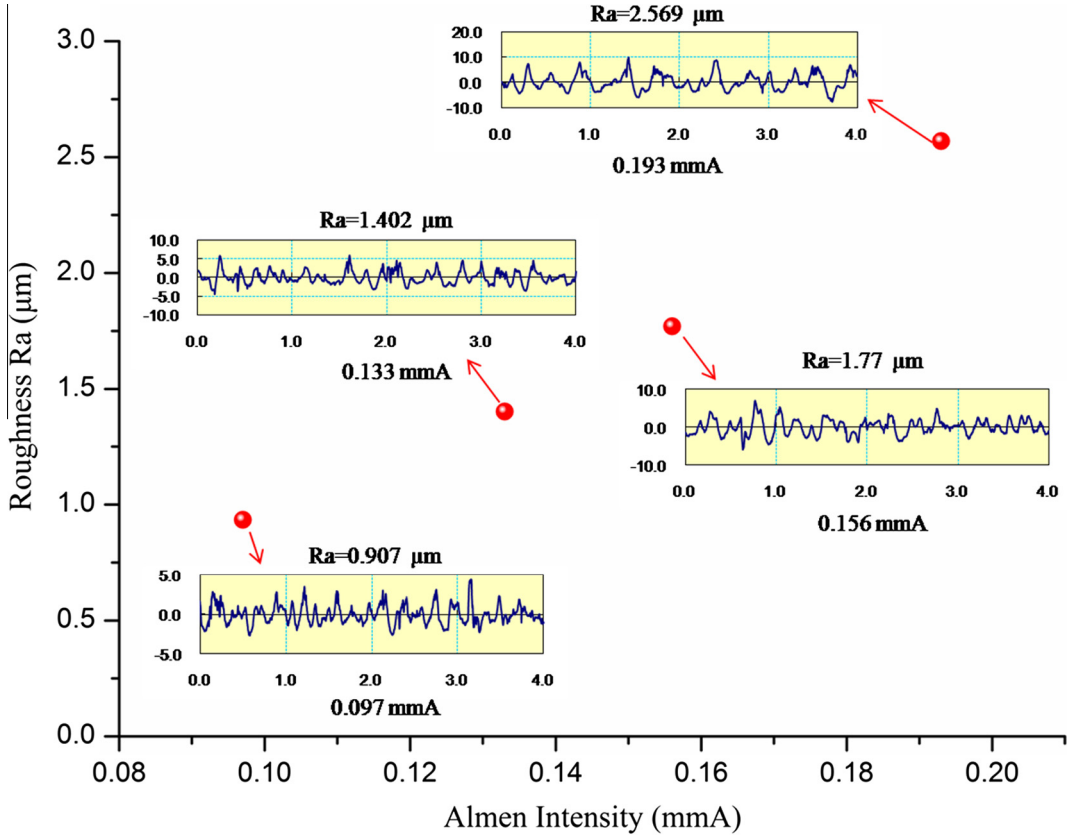

Fig. 10. Surface roughness (Ra) vs. Almen intensity. (For interpretation of the references to colour in this figure legend, the reader is referred to the web version of this article.)

$$Arc\ height\ (h_{PI-C}) = 2.57\ intensity - 0.087 \tag{4}$$

$$Arc\ height\ (h_{PEEK-U}) = 2.24\ intensity - 0.085 \tag{5}$$

$$Arc\ height\ (h_{PEEK-C}) = 3.01\ intensity - 0.120 \tag{6}$$

Fig. 10 shows the variation of surface roughness (Ra) with increasing the Almen intensity. It is found that with such increase, surface roughness values are increased, as expected.

3.3. Analysis of the deformation

Since the bending deformation of the strips is generated by the residual stress, the relationship between the curvature radius and the residual stress can be investigated. Fig. 11 shows the local face of the shot strips. The bending moment (M_p) caused by the residual compressive stress in the plastic deformation layer can be described as [16]:

$$M_p = \sigma_c \delta w \left(t - \frac{\delta}{2}\right) \Big/ 2 \tag{7}$$

where σ_c is the average compressive stress in the plastically deformed layer, δ is the thickness of the plastic deformation layer, w and t are the width and thickness of the strips respectively. At the same time, the bending moment (M_e) caused by the elastic deformation can be expressed as [24]:

$$M_e = \int_0^{t-\delta} \sigma(z)\left(\frac{t-\delta}{2} - z\right) w dz \tag{8}$$

Assuming that the elastic deformation layer is in a plane stress state and $\sigma_x = \sigma_y = \sigma$, the following equation can be obtained:

$$\sigma(z) = E\frac{\varepsilon(z)}{1-\upsilon} \tag{9}$$

where E is elastic modulus, υ is Poisson's ratio. Therefore, the Eq. (8) can be further expressed as:

$$M_e = \frac{EI_e}{(1-\upsilon)R} \tag{10}$$

where I_e is the moment of inertia, which can be obtained by Eq. (11) [25]:

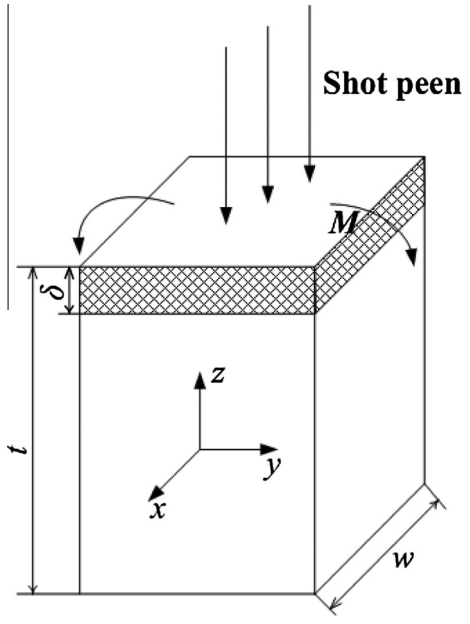

Fig. 11. Local face of the shot peening strips.

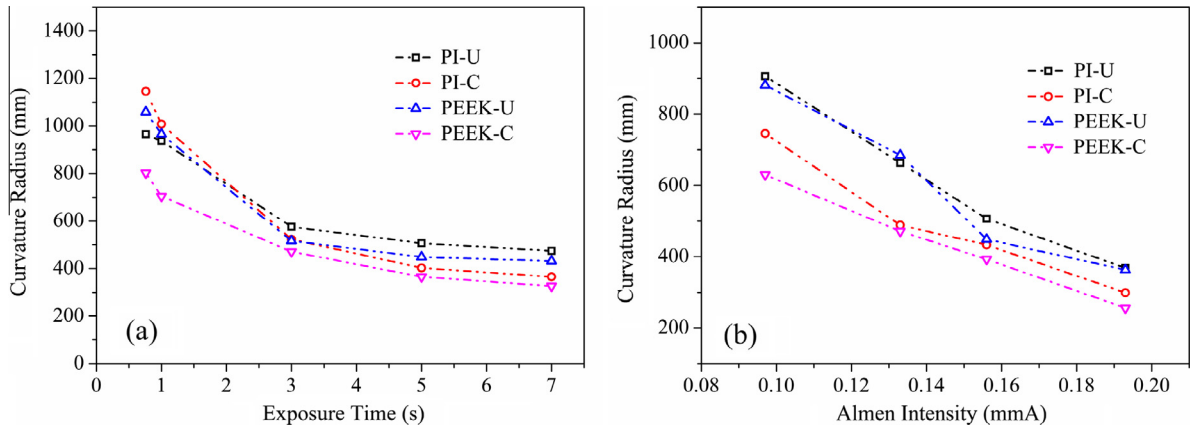

Fig. 12. (a) Experimental relationship between the curvature radius and the exposure time; (b) experimental relationship between the curvature radius and the Almen intensity. (For interpretation of the references to colour in this figure legend, the reader is referred to the web version of this article.)

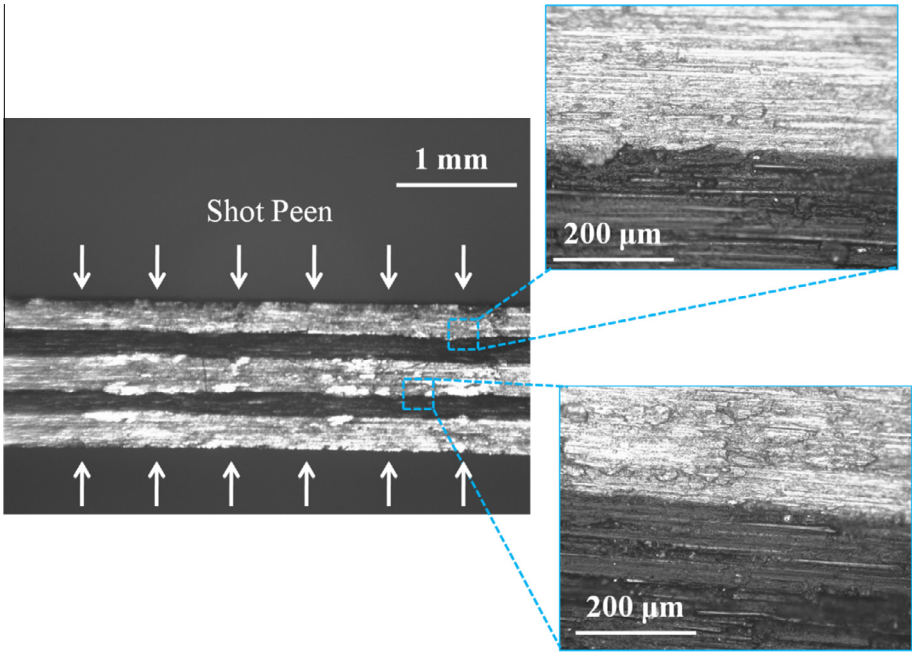

Fig. 13. Cross-section profile of the specimen after peening. (For interpretation of the references to colour in this figure legend, the reader is referred to the web version of this article.)

$$I_e = \frac{w(t-\delta)^3}{12} \tag{11}$$

Since the strips are statically balanced after shot peening, the bending moment caused by the residual compressive stress (M_p) is equal to the bending moment caused by elastic deformation (M_e). Thus, the curvature radius R can be calculated as follows:

$$R = \frac{E(t-\delta)^3}{6(1-\upsilon)\sigma_c\delta\left(t-\frac{\delta}{2}\right)} \tag{12}$$

Since $\delta \ll t$, Eq. (12) can be simplified as:

$$R = \frac{Et^2}{6(1-\upsilon)\sigma_c\delta} \tag{13}$$

Therefore, it can be concluded from the Eq. (13) that the curvature radius of the strip is directly proportional to the elastic modulus and inversely proportional to the residual stress as well as the thickness of the plastic deformation layer.

During the shot peening process, σ_c is increased with the increase of the exposure time. Hence, the curvature radius of the strip shows a decreasing trend. When the coverage reaches 100%, the surface layer of the metal almost reaches a fully plastic deformation state. The residual stress σ_c in the surface layer is stable after reaching fully plastic deformation state, causing the platform of the curvature radius as indicated in Fig. 12(a). Meanwhile, different responses after shot peening are observed in the FMLs with different fibre lay-ups according to Fig. 12(a) and (b). It is noted that the curvature radius of FML made with cross-ply lay-up is smaller than that of FML made with unidirectional layer-up after shot peening under the same peening parameter. FML made with unidirectional lay-up possesses higher elastic modules in the longitudinal direction than FML with cross-ply fibre lay-up, due to their higher fibre volume fraction in the fibre direction. Thus, it is more difficult for deformation to be generated in specimens with a higher elastic module, resulting in a relatively large curvature radius when going through the same peening process.

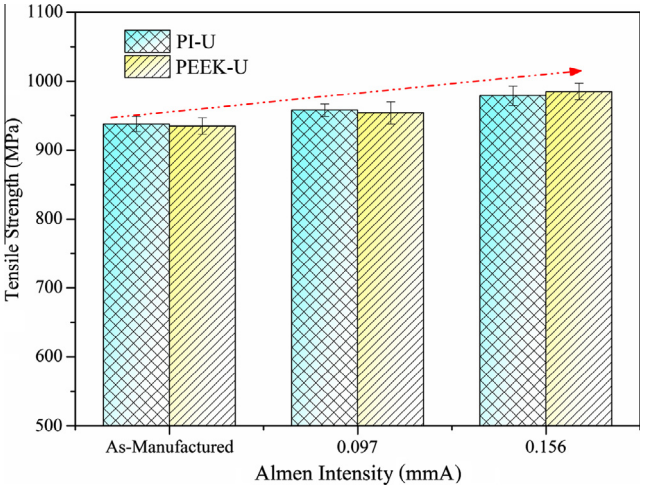

Fig. 14. Difference in tensile strengths of the specimens after peening. (For interpretation of the references to colour in this figure legend, the reader is referred to the web version of this article.)

3.4. Mechanical response after shot peening

Effects of the shot peening on the mechanical properties of FMLs need to be considered to guarantee the quality. As FMLs are super hybrid laminates composed by different layers, delaminations and micro-cracks are the most common defects which can deteriorate the mechanical properties of the FMLs. Fig. 13 presents the cross-section profile of the FML after shot peening. It is observed that the interfaces between the metal layers and the prepreg layers are continuous and well preserved. No visible delaminations and micro-cracks are generated after shot peening. Moreover, the results of the tensile tests shown in Fig. 14 clearly demonstrate the improvement of the tensile strength after shot peening process. It is known that shot peening can produce a high compressive stress in the surface layer of the metal. With the effect of the compressive stress, cracks caused by tensile stress are difficult to be generated in the surface, resulting in the enhancement of the mechanical properties of the metal layer [23]. Although the fibres carry most of the load in FMLs, the crack in metal can cause stress concentration. Cracks are not easy to generate in the surface metal layers after shot peening, resulting in the improvement of the mechanical properties of Ti/CFRP. Also, it can be deduced that the interfacial bonding within the FMLs is not damaged after shot peening with the employed parameters because the interfacial bonding determines the stress-transfer ability from the FML surface to the load-bearing fibres. Additionally, strips which are shot peened by using 0.156 mmA intensity show a higher tensile strength than that by using 0.097 mmA intensity.

4. Conclusions

Based on the work presented above, the following conclusions can be drawn:

(1) Bending deformation was successfully produced in Ti/CFRP laminates by using the shot peen forming technique. Extension of exposure time could increase the peening coverage and final arc heights of the FMLs strips. Surface roughness was increased initially with the extension of exposure time. Moreover, the final arc height of the FML strips was increased linearly with the augment of the applied Almen intensity.

(2) The relationship between the curvature radius and the peening parameters was analyzed. It was evident that the bending deformation was more difficult to be generated in the FMLs with unidirectional lay-up than that in FMLs with cross-ply lay-up.

(3) The shot peening could improve the mechanical properties of the FMLs rather than damage the interfacial bonding.

Acknowledgments

This work was supported by Funding of Jiangsu Innovation Program for Graduate Education; the Fundamental Research Funds for the Central Universities (No. KYLX_0258) and a Project Funded by the Priority Academic Program Development of Jiangsu Higher Education Institutions.

References

[1] Abouhamzeh M, Sinke J, Benedictus R. Investigation of curing effects on distortion of fibre metal laminates. Compos Struct 2015;122:546–52.
[2] Abdullah MR, Prawoto Y, Cantwell WJ. Interfacial fracture of the fibre–metal laminates based on fibre reinforced thermoplastics. Mater Des 2015;66:446–52.
[3] Cortes P, Cantwell WJ. The fracture properties of a fibre–metal laminate based on magnesium alloy. Compos B 2006;37(2):163–70.
[4] Hu YB, Li HG, Cai L, et al. Preparation and properties of fibre–metal laminates based on carbon fibre reinforced PMR polyimide. Compos B 2015;69:587–91.
[5] Pan L, Duan L, Zheng Z, et al. Surface characteristics and adhesive strength to polyetheretherketone of titanium electrografted with aryl diazonium salt. Mater Des 2016;95:555–62.
[6] Sinmazçelik T, Avcu E, Bora MÖ, et al. A review: fibre metal laminates, background, bonding types and applied test methods. Mater Des 2011;32(7):3671–85.
[7] Hu Y, Li H, Tao J, et al. The effects of temperature variation on mechanical behaviors of polyetheretherketone-based fiber metal laminates. Polym Compos 2016. http://dx.doi.org/10.1002/pc.24085.
[8] Zhong Y, Joshi SC. Response of hygrothermally aged GLARE 4A laminates under static and cyclic loadings. Mater Des 2015;87:138–48.
[9] Alderliesten R, Rans C, Benedictus R. The applicability of magnesium based fibre metal laminates in aerospace structures. Compos Sci Technol 2008;68(14):2983–93.
[10] Li H, Hu Y, Liu C, et al. The effect of thermal fatigue on the mechanical properties of the novel fibre metal laminates based on aluminum–lithium alloy. Compos A 2016;84:36–42.
[11] Li H, Hu Y, Xu Y, et al. Reinforcement effects of aluminum–lithium alloy on the mechanical properties of novel fibre metal laminate. Compos B 2015;82:72–7.
[12] Cortes P, Cantwell WJ. The impact properties of high-temperature fiber–metal laminates. J Compos Mater 2007;41(5):613–32.
[13] Kalyanasundaram S, DharMalingam S, Venkatesan S, et al. Effect of process parameters during forming of self reinforced–PP based fibre metal laminate. Compos Struct 2013;97:332–7.
[14] Dou X, Malingam SD, Nam J, et al. Finite element modeling of stamp forming process on fibre metal laminates. World J Eng Technol 2015;3(03):247.
[15] Dou X, Malingam SD, Nam J, et al. Finite element modeling of stamp forming process on thermoplastic-based fibre metal laminates at elevated temperatures. World J Eng Technol 2015;3(03):253.
[16] Sinke J. Manufacturing of GLARE parts and structures. Appl Compos Mater 2003;10(4–5):293–305.
[17] Gariépy A, Larose S, Perron C, et al. On the effect of the orientation of sheet rolling direction in shot peening forming. J Mater Process Technol 2013;213(6):926–38.
[18] Hong T, Ooi JY, Shaw B. A numerical simulation to relate the shot peening parameters to the induced residual stresses. Eng Fail Anal 2008;15(8):1097–110.
[19] Miao HY, Demers D, Larose S, et al. Experimental study of shot peening and stress peen forming. J Mater Process Technol 2010;210(15):2089–102.
[20] Russig C, Bambach M, Hirt G, et al. Shot peen forming of fibre metal laminates on the example of GLARE®. Int J Mater Form 2014;7(4):425–38.
[21] Cortes P, Cantwell WJ. The tensile and fatigue properties of carbon fibre-reinforced PEEK-titanium fibre-metal laminates. J Reinf Plast Comp 2004;23(15):1615–23.
[22] Gariépy A, Larose S, Perron C, et al. On the effect of the peening trajectory in shot peen forming. Finite Elem Anal Des 2013;69:48–61.
[23] Unal O, Varol R. Almen intensity effect on microstructure and mechanical properties of low carbon steel subjected to severe shot peening. Appl Surf Sci 2014;290:40–7.
[24] Luo Y, Deng D, Xie L, et al. Prediction of deformation for large welded structures based on inherent strain (mechanics, strength & structural design). Trans JWRI 2004;33(1):65–70.
[25] Hu Y, Zheng X, Wang D, et al. Application of laser peen forming to bend fibre metal laminates by high dynamic loading. J Mater Process Technol 2015;226:32–9.